CI&CEQ

Available on line at
Association of the Chemical Engineers *AChE*
www.ache.org.rs/CICEQ

Chemical Industry & Chemical Engineering Quarterly 17 (1) 45–52 (2011) CI&CEQ

MARIJA MIHAILOVIĆ[1]
ALEKSANDRA PATARIĆ[1]
ZVONKO GULIŠIJA[1]
DJORDJE VELJOVIĆ[2]
DJORDJE JANAĆKOVIĆ[2]

[1]Institute for Technology of Nuclear and other Mineral Raw Materials, Belgrade, Serbia
[2]Faculty of Tehcnology and Metallurgy, Belgrade, Serbia

SCIENTIFIC PAPER

UDC 543.545:66:669

DOI 10.2298/CICEQ100326052M

ELECTROPHORETICALLY DEPOSITED NANOSIZED HYDROXYAPATITE COATINGS ON 316LVM STAINLESS STEEL FOR ORTHOPAEDIC IMPLANTS

Hydroxyapatite is a widely used bioceramic material in implant coatings research because of its bioactive behavior when being deposited onto the metallic implant and compatibility with the human bones composition. The coating of nanosized hydroxyapatite was electrophoretically deposited on a blasted surface of stainless steel 316LVM samples at constant voltage, for different deposition times and subsequently sintered in both, vacuum and argon atmosphere, at 1040 and 1000 °C, respectively. Although sintering temperatures needed to achieve highly dense coatings can cause HAp coating phase changes, the possibility to obtain a bioactive coating on 316LVM substrate, without the coatings phase changes due to the nature of the used stoichiometric nanostructured hydroxyapatite is presented in this work. The thermal stability of the used HAp powder was assessed by DTA-TG analyses over the temperature range of 23-1000 °C, i.e., at the or nearby experimental sintering temperature. The microstructure characterization was accomplished using SEM, while phase composition was determined using XRD.

Key words: electrophoretic deposition; hydroxyapatite; 316LVM stainless steel; coatings.

Investigations on surgical hip implants surface improvement through the possibility of depositing a biocompatible coating started a couple of decades ago [1-9]. Conventional metallic materials for hip implants, besides the 316LVM stainless steel, are titanium- and cobalt/chromium-based alloys. Although bioinert, due to their corrosion resistance, they are not biocompatible. However, their surface can be coated with a biocompatible material, such as hydroxyapatite (HAp) [$(Ca_{10}(PO_4)_6(OH)_2)$]. HAp is chemically identical with the mineral constituent of bones and teeth, providing its biocompatibility. This material's limitations are, however, weak tensile strength and low fatigue resistance for long term loadings, if used alone [1,10]. If hydroxyapatite is deposited onto the surgical implant, besides biocompatibility, the bioactivity could also be achieved, so that intergrowth with bones enables firm attachment of the implant to the bone. This provides long-lasting and mechanical stable non-cemented prosthesis, thus eliminating the need for another surgery after certain utilization period.

During the last decades of research, a number of technological methods for HAp coatings deposition on metallic implants were developed, such as: ion beam deposition [11] plasma spraying [5,6], sputtering, sol-gel coating, biomimetic methods and electrophoretic deposition [2-4,7-9,12-16]. The major problems related to high temperature processes, such as plasma spraying, besides the HAp decomposition, are associated with difficulties to produce a uniform coating over the complex substrate geometry. To overcome these restrictions the electrophoretic deposition (EPD) of HAp on metal substrates is used. EPD is a quite efficient and inexpensive method to obtain dense and uniform coatings on metal substrates, even with complex geometries [14]. The other advantages of this method are high purity of formed coating on metallic substrate, the possibility of obtaining the desired coating thickness and relatively simple process control by influencing parameters variation [15].

The majority and a kind of continuity in publishing investigation results concerning surface enhancement refer to titanium based materials [2,5,6,9-13,17], but there are also those referring to the stainless steel

Correspondening author: M. Mihailović, Institute for Technology of Nuclear and other Mineral Raw Materials, Franše d'Eperea 86, 11 000 Belgrade, Serbia.
E-mail: m.mihailovic@itnms.ac.rs
Paper received: 26 March, 2010
Paper revised: 28 July, 2010
Paper accepted: 8 September, 2010

[3,9,14-16,18,19]. Both the steel and titanium alloy surgical implants, although structurally and mechanically superior, as well as corrosion resistant, are susceptible to local corrosion in the human body, releasing metal ions into the surrounding body tissue and fluids. Through surface modification their biocompatibility can be achieved, keeping the benefit of their mechanical properties.

316LVM stainless steel is commonly used as an implant material due to its mechanical properties (strength, ductility), corrosion resistance, and low cost - which can sometimes be the main preference [15]. Since the substrate with deposited HAp coating should be subjected to relatively high sintering temperatures, the advantage of stainless steel compared to titanium alloys is a better thermal expansion coefficient match with hydroxyapatite, *i.e.*, the thermal expansion coefficient of the coating should be somewhat lower than that of the substrate [9,8]. Such thermal coefficients correlation should result in compressive residual stresses in the coating, thus inhibiting the cracking during cooling.

Sintering is an unavoidable, but critical stage, because the coating must be densified after the deposition, and it occurs at temperatures of at least 1200 °C for the most of commercially available HAp powders [4,20-24]. During the sintering stage the coating densificates, but such a high sintering temperature can cause the thermal decomposition of the coating itself, as well as the degradation of the mechanical properties of the metal implant [2,9]. There are studies in which it was demonstrated that the tensile strength of 316LVM stainless steel was unaffected by the temperatures up to 1050 °C [8]. Therefore, these authors [8] suggested that concerning the metal implant mechanical properties retention, the densification temperatures should not exceed 1050°C. With regard to HAp-metal interfacial decomposition reaction, the same authors showed that HAp decomposes at much lower temperatures if being in contact with a metal. So, in contact with 316LVM stainless steel the typical HAp decomposition temperature of 1300°-1400 °C is reduced to ~950 °C [7,8]. Therefore, the lowering of the sintering temperature is desirable in HAp coating/metal system [18]. Minimization of the HAp densification temperature requires the use of HAp powders with maximal specific surface area, so only with as-precipitated uncalcined powders the 100% density plateau could be approached [18]. The present work investigated the nanosturctured HAp powder obtained by a novel modified spray-dry method. Having in mind the proven stability of the used HAp powder [21], it is decided to carry out the experiments at the temperatures above those reported for a HAp decomposition, but limited with the metal substrate properties.

The important requirement concerning the HAp powder was its stoichiometric Ca/P ratio, with required chemical and phase composition, which was approved earlier [21,22]. Presented here is an attempt to maintain the stoichiometric Ca/P ratio after such HAp powder is deposited on 316LVM substrate and deposited coating is sintered at temperatures as high as metal substrate could resist the change in terms of structural and mechanical properties.

Furthermore, sintering had to be performed in a protective atmosphere because the presence of oxygen could lead to metal substrate/HAp coating interface oxidation which results in weak bonding of ceramic coating to the metallic substrate [9,15,19].

The aim of this work was to investigate the possibility to obtain a bioactive coating, made of non commercial home-synthesized nanostructured HAp powder on 316LVM substrate.

EXPERIMENTAL

The used HAp powder is synthesized by a novel modified precipitation method which is improved by spray-drying at 120±5 °C, as described elsewhere [21]. The Ca/P ratio of 1.67±0.01 was determined by ICP analyses.

The characterization of the powder, including morphology and particle size, was accomplished using a transmission electron microscope (Philips EM 420) and scanning electron microscope (Jeol T-20), while phase composition was evaluated by an X-ray diffractometer (Philips PW1710) with CuKα radiation and curved graphite monochromator, measuring angle 2θ in the range from 20 to 70° and step scan of 0.02°. The same diffractometer was used for X-ray diffraction (XRD) analysis of deposited and sintered HAp coatings. The morphology of deposited and sintered HAp coatings was examined with a scanning electron microscope (Jeol JSM 5800).

In order to estimate the thermal stability of the used HAp against the sintering temperature, the DTA--TG analyses of the HAp powder were carried out using a NETZCH STA 409EP device, at heating degree of 10 °C/min in the temperature range 23-1000 °C, *i.e.*, up to the experimental sintering temperature.

The stainless steel 316LVM plates commonly used for hip implants, with dimensions of 40 mm×15 mm×2 mm, were used as both cathode and anode for the electrophoretic deposition process.

Metallic specimens were blasted with commercial garnet (0.1-0.4 mm), at 90° blasting angle, with working distance of 25 cm and air pressure of 0.6 N/mm^2. The mean surface roughness, *Ra*, was 6.3 μm, and it was determined using a T-200 Handheld roughness tester. Blasting enables a clean surface; nevertheless the blasted specimens were then rinsed with acetone and distilled water. Afterwards, they were dried at room temperature and stored in a desiccator before the EPD procedure.

Suspension of HAp particles was performed by agitation using magnetic stirrer of 0.5 g of the HAp powder in 100 ml of ethanol. Ethanol was reported to be the suitable medium for this purpose [8]. For the suspension stability, the 10% HCl was added until pH 2.00 was reached.

Electrophoteric deposition was carried out in a self-made EPD cell, consisting of 150 ml glass beaker and a holder for fixing electrodes at a distance of 15 mm. The electrodes were parallel to each other connected to a MA410 3DC power supply (Iskra). Both the cathode and anode were of the same dimensions. The deposition electrode was the cathode.

The electrophoretic deposition of HAp particles on the 316LVM stainless steel substrate plates was performed at the constant voltage of 60 V, since it was determined to be optimal for EDP of HAp deposition onto the 316LVM steel [19].

The deposition times were 30 and 60 s. The coated specimens were drying at room temperature in the desiccator before sintering. The subsequent heat treating for sintering was carried out in argon and in vacuum.

Specimens were taken one after the other into an electric furnace, at 200 °C, previously degassed for 1 h, and heated up to 1000 °C in argon atmosphere, with heating rate of approximately 10 °C/min, while the reported heating rates varied from approximately ten times slower, equal or up to five times faster [12,13,19]. They were held at the sintering temperature for 1 h, cooled in the furnace and taken out.

For vacuum sintering, all the specimens were taken at the same time into a furnace chamber, each in separate holder. The heating rate was approximately 10 °C/min. The sintering temperature of 1040 °C was reached at the vacuum of 10^{-4} mbar. Samples were held there for 1 h and slowly cooled, with the furnace. This was the highest temperature that could be reached in the furnace (Ipsen), while the vacuum enabled protecting atmosphere. Nevertheless, these sintering temperatures are at the lower level of the HAp sintering temperature range, but at the upper limit temperatures regarding the retaining of metal substrate properties.

The HAp powder was examined by DTA-TG NETZCH STA 409EP for evaluation of its thermal stability, while deposited and sintered HAp coatings were examined by XRD Philips PW1710 and SEM Jeol JSM 5800.

RESULTS AND DISCUSSION

The estimation of the thermal stability of the used HAp powder against the sintering temperature was carried out by the DTA-TG analyses (Figure 1).

In Figure 1, the TG curve demonstrates a rapid weight loss up to 200 °C and a continuous slight weight loss above 200 °C. Accordingly, the DTA curve shows an endothermic change at the 112 °C caused by humidity release, while over the temperature range of 200-1000 °C there was no significant DTA change accompanied to the TG change. The DTA curve has a slight exothermic tendency, which does not indicate any phase change, and the TG curve in the temperature range of 800-1000 °C, has the relative change of -0.62%. This is the temperature range in which the phase transformation of HAp into the detrimental β--TCP (tricalcium phosphate) is reported to occur when HAp is deposited on the 316LVM steel surface, due to HAp/metal interfacial decomposition reaction [7-9]. In contact with 316LVM stainless steel, the typical HAp decomposition temperature of 1300-1400 °C is reduced to ~950 °C [7,8].

Usually, the DTA endothermic peak accompanied with the TG weight loss may be due to the decomposition of HAp into the TCP. This, however, should be in accordance with XRD pattern and TPC peaks on it [25].

Here obtained results may be considered in favour of the HAp powder thermal stability over the temperature range of 23-1000 °C, and at the experimental sintering temperature. The absence of β-TCP peaks at XRD pattern of the HAp coatings can also be interpreted in favour of the HAp powder stability in contact with 316LVM.

Figure 2 presents the XRD pattern of the HAp nano-powder, exhibited peaks corresponding to the hydroxyapatite phase, indicating a low crystallinity. Figures 3a and 3b showing XRD patterns of electrophoretically deposited HAp powder for 30 s, and subsequently heat treated for sintering in vacuum (Fig. 3a) and in Ar atmosphere (Fig. 3b), also indicate a very low crystallinity. The only peaks registered at Figures 2 and 3b were those corresponding to the hydroxyapatite phase. All the peaks perfectly matched the

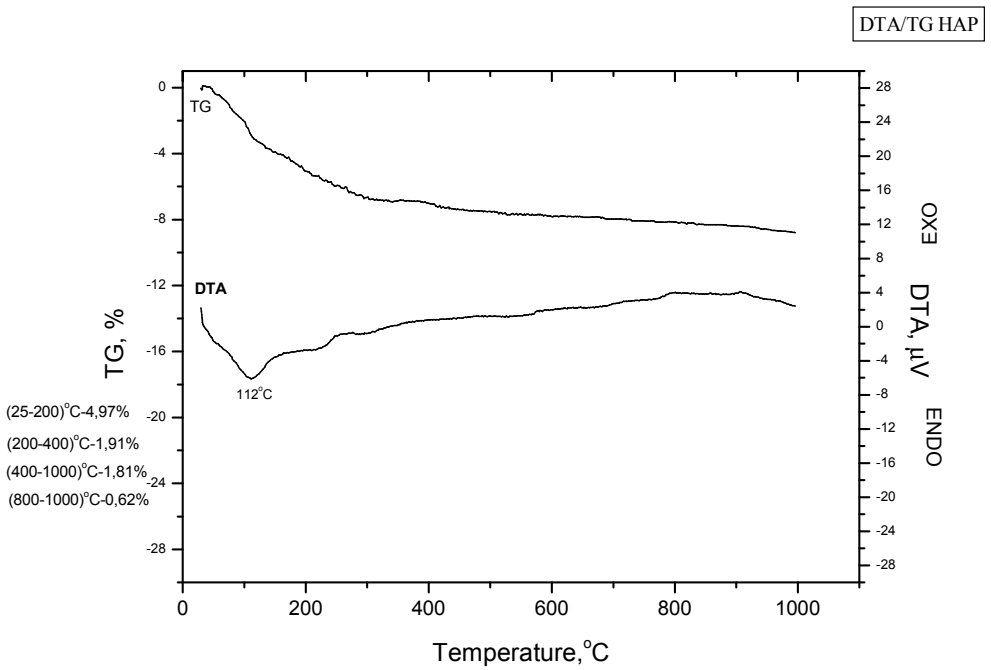

Figure 1. DTA-TG curves of the HAp powder.

JCPDS pattern 9-432 for HAp, suggesting that the pure HAp powder was obtained [21] and that the phase composition of the coating after EPD and sintering processes was the same as that for the starting powder (Figure 3b). Since the compatible peaks were recognized at XRD patterns of the powder and of the coating, it may be concluded that there was no phase transformation during the sintering process.

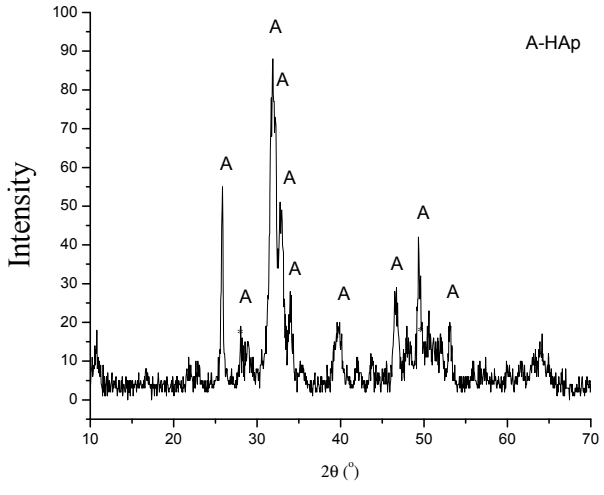

Figure 2. XRD pattern of HAp powder.

The exhibition of wide XRD peaks from Figure 2 could be due to the low crystallinity or the result of the crystal size effect [22,23]. According to suggested calculation [22] the fraction of crystalline phase in the HAp powders can be evaluated from the intensity ratio of the characteristic diffraction peaks (the intensity of (300) diffraction peak and the intensity of the hollow between the (112) and (300) diffraction peaks of HAp). The evaluated degree of crystallinity for samples used in [22] was higher than expected from the XRD pattern appearance. Accordingly, the wide peaks at the XRD pattern of the HAp powder used in this investigation could be caused by very small, *i.e.*, nanosized rod-shaped HAp powder particles, 50-100 nm in size, which were observed in previous TEM image analysis of the here used HAp powder [21]. Besides influencing the low crystallinity, this nanostructured starting powder may favor the densification process and their high thermal stability, *i.e.*, the absence of thermal decomposition products [8,18-20,22].

The HAp peaks were not such a wide in Figures 3a and 3b, meaning that sintered powder has a better crystallinity. The γ-Fe peak on the XRD pattern, Figure 3a, of the HAp coating sintered in vacuum at 1040 °C is the peak originating from the substrate, indicating that the coating is not compact enough. For samples electrophoretically deposited for 60 s and subsequently heat treated for sintering in vacuum and Ar atmosphere, thicker coating was obtained, but XRD patterns were analogue to these for shorter deposition time, *i.e.*, vacuum heat treated samples exhibited γ-Fe peak originating from the substrate. Since the sintering temperature in vacuum was higher, it may be assumed that the thermal stresses during sintering may have caused this cracking.

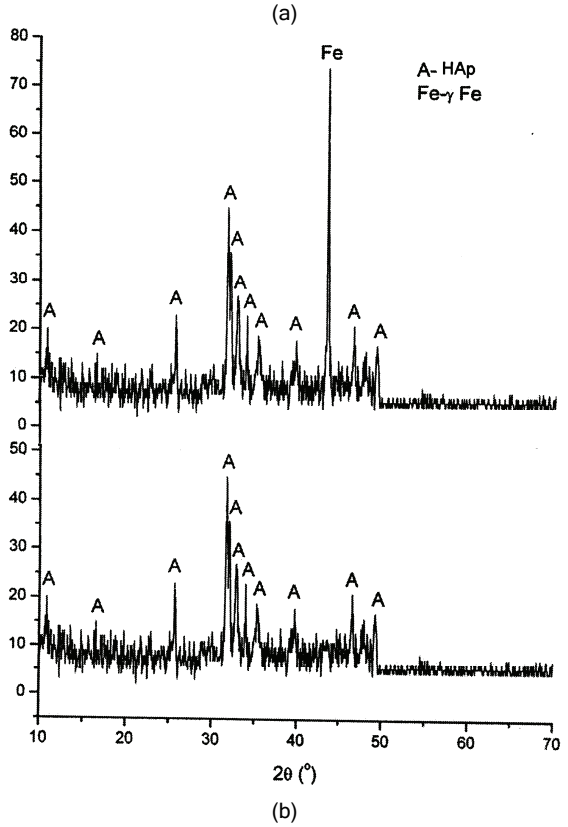

Figure 3. XRD patterns of HAp coatings, sintered in vacuum (a) and Ar-atmosphere (b).

There are several reported methods for precipitation of non-commercial self-made HAp powders and different morphology of HAp particles, depending on the powder obtaining method [18]. The morphology has a significant impact on the electrophoretic coating quality, namely the best coatings were obtained by the rounded particles, the worst was with platy particles, while acicular particles (185nm), similar to here used powder with nanosized rod-shaped particles (sizing from 50 to 100 nm) resulted in some cracking of the coating during drying. The shrinkage due to drying could be minimized by the use of regularly shape particles that can pack more efficiently. The nano-rods in the used HAp powder are almost one order of magnitude smaller than those in reported investigation, although with rather similar aspect ratio.

Electrophoretic deposition is achieved by the motion of charged particles toward an electrode under applied electric field. It was found that deposit weight and thickness increased with deposition voltage and deposition time, until the saturation was reached and voltage drop resulted from increased coating thickness [3] For the condition of the suspension with low solid concentration, the electrophoretic velocity is mainly a function of the electric field and the particle size [3,12,13]. When the electric field is constant, the preferential deposition of finer particles can be expected due to their higher mobility comparing to the larger particles [12]. Knowing that the closest to the substrate the finer particles can be observed and that with shorter deposition time, only the very fine nanoparticles were reached the substrate surface, it can be assumed that the coating formed for shorter deposition time of 30 s is made of very fine particles with low susceptibility to cracking.

The absence of the γ-Fe peak or the peaks corresponding to detrimental structure phases, namely tricalcium phosphate (TCP) is evident in the presented XRD pattern of a coating sintered in Ar atmosphere at 1000 °C, Figure 3b. The absence of γ-Fe peak indicates that coating covers the substrate continuously, without pores or cracks, through which the peak originated from the substrate could be recorded, as was the case in the previous sintering case. This also means that the Ca/P ratio of 1.67±0.01 remains unchanged, favorizing the bioactivity of the coating.

The surface morphologies, obtained by SEM, of electrophoretically deposited coatings, both for 30 and 60 s of deposition, and subsequently heat treated in vacuum as described previously, are presented in Figures 4 and 5, respectively.

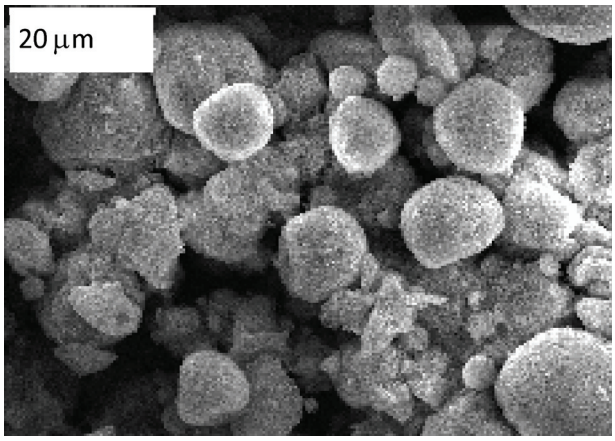

Figure 4. Surface morphology of the 30 s EPD-coated and in vacuum heat treated sample.

Since EPD processes were carried out at constant voltage, the coating thickness was influenced by elapsed deposition time. It is proven that at higher applied voltages and for longer deposition times, the coating thickness increases giving porous and cracked coating, *i.e.*, the coarser outer deposited particles affect the coating integrity [12]. The coatings obtained for shorter deposition times, such as 30 s, are thinner but more compact compared to those obtained for longer deposition times, such as 60 s. Namely, it can

be seen from the Figure 4, obtained for 30 s EPD--coated and in vacuum sintered sample, that the certain changes have occurred at the agglomerates surface, but the sintering may have occurred in a low degree or not at all. As can be seen from the SEM acquired morphology in Figure 5, for a specimen obtained after electrophoretic deposition for 60 s and vacuum heat treated, the outer layer of agglomerated clusters has cracks through which the inner layer of finer and sintered particles is noticeable. The coating layer closest to the substrate was observed to be continuous, whereas the outer coating layers were porous or cracked, Figure 5.

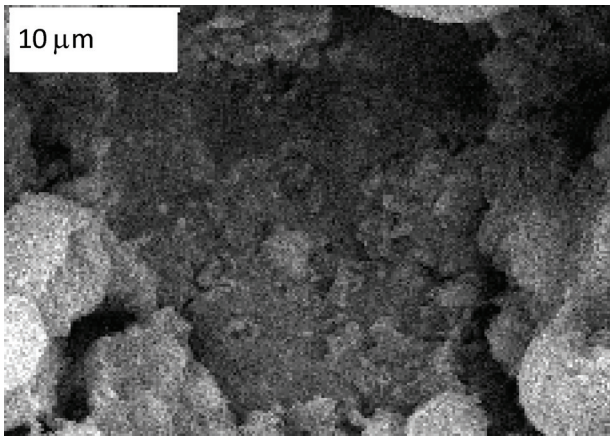

Figure 5. Surface morphology of the 60 s EPD-coated and in vacuum heat-treated sample.

Since it was proven that the adequate densification, and the associated high degree of shrinkage, can lead to cracking because the shrinkage of dense coatings causes tensile stresses and therefore cracking [8], it can be assumed that at higher sintering temperature of 1040 °C, in the vacuum furnace, the effect of densification took place which, accompanied with higher tensile stresses caused cracking.

It can be assumed that for a longer ultra-sound suspension treatment, it would be possible to obtain uniformly distributed particles and the coating could have been better sintered.

Figure 6 presents the morphology of a sample EPD-coated for 30 s, and afterwards sintered in Ar atmosphere. Here, the morphology of sintered coating is visible not only at the agglomerates at the surface as for 30 s EPD and vacuum sintered, but all over the same visible area at the same magnification.

For specimens sintered in Ar atmosphere the obtained coating is comparatively uniform and free of cracks, which may be concluded by both XRD and SEM. At the XRD patterns of these Ar-sintered samples, just HAp reflections are detected. The surface morphology obtained by SEM of 30 s EPD-coated and in Ar heat treated sample, under very high magnification, such as x17000, is presented in Figure 7. The agglomerates made of sintered primary HAp powder nanoparticles deposited onto the 316LVM stainless steel and heat treated in Ar-atmosphere at 1000 °C for 1 h, are visible.

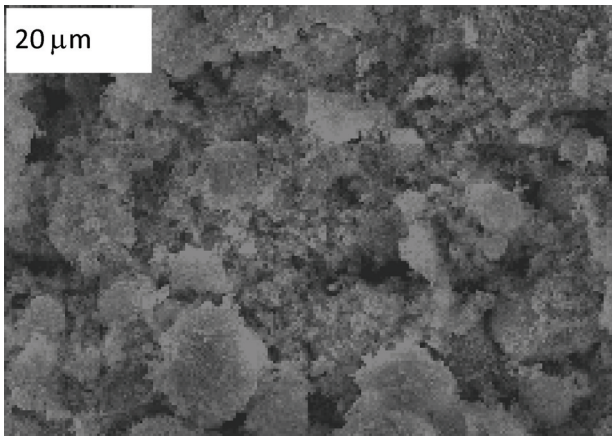

Figure 6. Surface morphology of the 30 s EPD-coated and in Ar sintered sample.

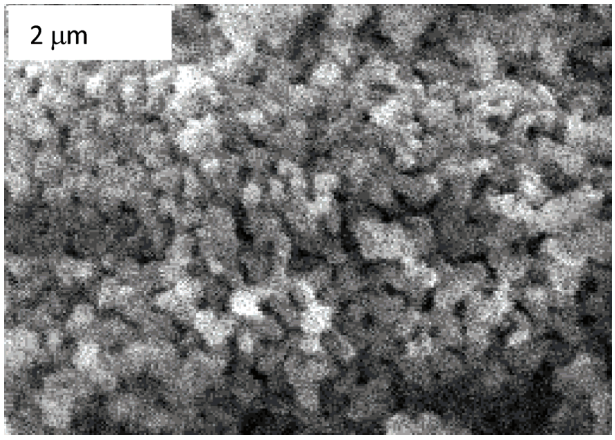

Figure 7. Surface morphology of the 30 s EPD-coated and in Ar sintered sample - sintered nanoparticles of primary HAp powder.

Contrary to the XRD patterns obtained for specimens sintered in Ar atmosphere, the XRD pattern for vacuum sintered specimens has a γ-Fe reflection, indicating the presence of pores or cracks of the coating. These cracks could be probably caused by higher densification occurred in this case, because of the higher sintering temperature as discussed above, and the thermal stresses during sintering due to high heating rate. Since the difference in the thermal expansion coefficient between these two materials should not be challenging [8], it may be concluded that the heating rate should be much slower. Particularly, when the

thermal expansion coefficient of the ceramic coating is similar or lower than for the metal substrate, as in the case with HAp and 316LVM stainless steel, than the residual stresses in the coating are compressive, inhibiting the cracking.

At the same time, it can be concluded that the metal catalyzed decomposition of the HAp coating was not observed here, having in mind the assessed thermal stability of the powder by DTA-TG and since the XRD detected reflections belong to the original HAp and γ-Fe, originating from the substrate.

Further investigations should be aimed to overcome this shrinkage problem by depositing an intermediate layer or a multilayer using this nanosized HAp powder, together with the slower heating rate. This approach was already applied through investigations [8,13,17,18] or by a dynamic voltage experiments [12]. Some investigations were also undertaken to lower the sintering temperature of EPD coatings [8,23,24], and it was shown that the nanostructured coatings enabled new breakthroughs in the area of electrophoresis [8] and the coatings were deposited at conditions which were thought to be inappropriate. Since the investigations were carried out mostly using homemade powders, each powder and depositing procedure has its specific conditions and methods in overcoming the coating disadvantages.

CONCLUSIONS

The thermal stability of the used HAp powder was assessed by DTA-TG analyses and did not show any characteristic change over the temperature range of 23-1000 °C, *i.e.*, at the or nearby experimental sintering temperature.

The absence of peaks of detrimental high-temperature phase at XRD pattern of the HAp coatings can also be interpreted in favor of the HAp powder stability in contact with 316LVM, possibly due to the use of nanostructured stable, stoichiometric HAp powder.

The XRD patterns of the nanosized HAp powder showed the presence of characteristic HAp peaks, while the detrimental high temperature phase due to decomposition of HAp was not registered.

The XRD patterns for both, shorter and longer deposition time, in vacuum sintered samples exhibited HAp peaks accompanied by a γ-Fe peak, regardless the coating thickness, probably due to high heating rate and higher sintering temperature, than that for sintering in Ar-atmosphere. This may have caused higher thermal stresses, although the cooling rate was rather slow. If the suspension was ultrasonically agitated, the particles distribution would have been much better and hence the coating might have been more compact.

XRD patterns of the coatings sintered in Ar-atmosphere have shown just characteristic HAp peaks, meaning that comparatively continuous and crack-free HAp coatings were produced after sintering in Ar atmosphere at 1000 °C for 1 h, at lower sintering temperature than in vacuum furnace.

At the SEM morphologies the coating layer closest to the substrate was observed to be continuous, whereas the outer coating layers were porous or cracked. To overcome this problem, experiments should be carried out by depositing an intermediate layer or a multilayer using this nanosized HAp powder.

Finally, the use of the stable, stoichiometric HAp powder, synthesized by a method which produced the nanosized rod-shaped particles, enabled obtaining the continuous HAp coatings onto the 316LVM stainless steel, where the only inherent ceramic phase is HAp.

Acknowledgement

The authors wish to acknowledge the financial support from the Ministry of Science and Technological Development of the Republic of Serbia through the project MHT 19015.

Nomenclature

HAp – Hydroxyapatite
EPD – Electrophoretic deposition
316LVM – According to AISI, the 316 steel low vacuum melted
SEM – Scanning electron microscopy
XRD – x-Ray diffractogram
pH – pH Value, a measure of acidity
TEM – Transmission electron microscopy
TCP - Tricalcium phosphate
γ-Fe - Fe with γ-type lattice (face centered cubic lattice).

REFERENCES

[1] W. R. Lacefield, in Bioceramics: Materials Characteristics Versus *in Vivo* Behavior, P. Ducheyne and J.E. Lemons, Ed., New York Academy of Science, New York, 1988, p. 73-80

[2] P. Ducheyne, S. Radin, M. Heughebaert, J.C. Heughebaert, Biomatterials **11** (1990), 244-254

[3] I. Zhitomirsky, L. Gal-Or, J. Mater. Sci. Mater. Med. **8** (1997) 213-219

[4] A. J. Ruys, C. C. Sorell, A. Brandwood, B. K. Milthrope, J. Mater. Sci. Lett. **14** (1995) 744-747

[5] R. B. Heimann, H. Kurzweg, D.G. Ivey, M. L. Wayman, J Biomed Mater Res (Appl. Biomater.) **43** (1998) 441–450

[6] H. Kurzweg, R. B. Heimann, T. Troczynski, M. L. Wayman, Biomaterials **19** (1998) 1507-1511

[7] M. Wei, A. J. Ruys, B. K. Milthrope, C. C. Sorrell, J. Biomed. Mater. Res. A **45** (1999) 11-19

[8] M. Wei, A. J. Ruys, M. V. Swain, S. H. Kim, B. K. Milthrope, J. Mater. Sci. Mater. Med. **10** (1999) 401-409

[9] M. Wei, A. J. Ruys, B. K. Milthorpe, C. C. Sorell, J. H. Evans, J. Sol-Gel Sci. Technol. **21** (2001) 39-48

[10] C. Y. Tang, P. S. Uskokovic, C. P. Tsui, Dj. Veljovic, R. Petrovic, Dj. Janackovic, Ceram. Int. **35** (2009) 2171-2178

[11] J. M. Choi, H. E. Kim, I. S. Lee, Biomaterials **21** (2000) 469-473

[12] X. Meng, T. Y. Kwon, K. H. Kim, Dent. Mater. J. **27** (2008) 666-671

[13] D. Stojanovic, B. Jokic, Dj. Veljovic, R. Petrovic, P. S. Uskokovic, Dj. Janackovic, J. Eur. Ceram. Soc. **27** (2007) 1595-1599

[14] S. Kannan, A. Balamurugan, S. Rajeswari, Mat. Lett. **57** (2003) 2382-2389

[15] T. M. Sirdhar, U. Kamachi Mudali, M. Subbaiyan, Corros. Sci. **45** (2003) 237-252

[16] N. Eliaz. T.M. Sridhar, U. K. Mudali, B. Raj, Surf. Eng. **21** (2005) 1-5

[17] A. Stoch, A. Brožek, G. Kmita, J. Stoch, W. Jastrzebski, A. Rakowska, J. Mol. Struct. **596** (2001) 191-200

[18] M. Wei, A. J. Ruys, B. K. Milthrope, C. C. Sorrell, J. Mater. Sci. Mater. Med. **16** (2005) 319-324

[19] M. Javidi, S. Javadpour, M. E. Bahrololoom, J. Ma, Mater. Sci. Eng. C **28** (2008) 1509-1515

[20] Dj. Veljović, I. Zalite, E. Palcevskis, I. Smiciklas, R. Petrović, Dj. Janaćković, Ceram. Int. **36** (2010) 595-603

[21] Dj. Veljović, B. Jokić, R. Petrović, E. Palcevskis, A. Dindune, I. N. Mihailescu, Dj. Janaćković, Ceram. Int. **35** (2009) 1407-1413

[22] E. Landi, A. Tampieri, G. Celotti, S. Sprio, J. Eur. Ceram. Soc. **20** (2000) 2377-2387

[23] X. F. Xiao, R. F. Liu, Mat. Lett. **60** (2006) 2627-2632

[24] B. Baufeld, O. van der Biest, H. J. Raetzer-Scheibe, J. Eur. Ceram. Soc. **28** (2008) 1793-1799

[25] M. Aizawa, H. Ueno, K. Itatani, I. Okada, J. Eur. Ceram. Soc **26** (2006) 501-507.

MARIJA MIHAILOVIĆ[1]
ALEKSANDRA PATARIĆ[1]
ZVONKO GULIŠIJA[1]
DJORDJE VELJOVIĆ[2]
DJORDJE JANAĆKOVIĆ[2]

[1]Institut za tehnologiju nuklearnih i drugih mineralnih sirovina, Beograd, Srbija
[2]Tehnološko-metalurški fakultet, Beograd, Srbija

NAUČNI RAD

ELEKTROFORETSKO TALOŽENJE PREVLAKA HIDROKSIAPATITNOG NANO-PRAHA NA ČELIK ZA IZRADU ORTOPEDSKIH IMPLANTATA 316LVM

Hidroksiapatit se široko koristi kao keramički biomaterijal zbog svoje bioaktivnosti koju ispoljava kada se u vidu prevlake nanese na metalni implantat, kao i zbog kompatibilnosti sa sastavom ljudskih kostiju. Prevlake hidroksiapatitnog nano-praha elektroforetski su istaložene na peskiranu površinu uzoraka od nerđajućeg 316LVM čelika, pri konstantnom naponu i za različito vreme taloženja, a potom sinterovane u vakuumu na 1040 °C i u atmosferi argona na 1000 °C. Premda visoke temperature sinterovanja, koje su neophodne kako bi se dobile kompaktne prevlake velike gustine, mogu da dovedu do faznih promena kod hidroksiapatita, u ovom radu je pokazano da je na supsrtatu od 316LVM čelika moguće dobiti bioaktivne prevlake u kojima nije došlo do fazne promene zahvaljujući prirodi korišćenog hidroskiapatitnog nano-praha stehiometrijskog sastava. Visokotemperaturna stabilnost korišćenog HAp praha potvrđena je DTA-TG analizom u temperaturnom opsegu 23-1000 °C, tj. na temperaturama na kojima su rađeni eksperimenti sinterovanja. Mikrostrukturna karakterizacija nanetih prevlaka urađena je korišćenjem SEM, dok je za određivanje faznog sastava korišćena XRD analiza.

Ključne reči: elektroforetsko taloženje; hidroksiapatit; nerđajući čelik 316LVM; prevlake.